



Istanbul Bridge Conference  
August 11-13, 2014  
Istanbul, Turkey

# ANALYSIS OF CRACKING BEHAVIOUR FOR REINFORCED CONCRETE CURVED BOX GIRDER BRIDGES

Yiqiang Xiang<sup>1</sup> and Jianwu Xu<sup>2</sup>

## ABSTRACT

Mechanical behavior of curve reinforced concrete box girder bridges from elastic, cracking, deflection increasing to failure stage is extremely complex under load. A 3D solid element model of a typical cracking curved concrete continuous box girder bridge in a highway ramp road was established. The whole behavior from cracking to failure of the bridge was analyzed. The cracking of curved box girder bridges with different curvature radius, support style and reinforced bar arrangement, etc. parameters were explored. The numerical results showed that the proposed analysis model was effective for calculating nonlinear behavior after cracking of curve concrete box girder bridges. There is good agreement between the location and distribution of the predicted crack and survey results of actual bridge site. Mechanical behavior of curved box girders can be improved by taking measures such as suitably arranging bearings, reasonably setting pre-eccentricity distance of bearings, increasing reinforcement ratio.

---

<sup>1</sup>Professor, Dept. of Civil Engineering, Zhejiang University, Cyrus Tang Center for Sensor Materials and Applications, Zhejiang University, Hangzhou, 310058, China; Dept. of Civil Engineering, Zhejiang University City College, 310015, China

<sup>2</sup> Engineer, Design Institute of Highway, Zhejiang Transportation Investment Group Co., Ltd., Hangzhou, 311200, China

# Analysis of Cracking Behaviour for Reinforced Concrete Curved Box Girder Bridges

Yiqiang Xiang<sup>1</sup> and Jianwu Xu<sup>2</sup>

## ABSTRACT

Mechanical behavior of curve reinforced concrete box girder bridges from elastic, cracking, deflection increasing to failure stage is extremely complex under load. A 3D solid element model of a typical cracking curved concrete continuous box girder bridge in a highway ramp road was established. The whole behavior from cracking to failure of the bridge was analyzed. The cracking of curved box girder bridges with different curvature radius, support style and reinforced bar arrangement, etc. parameters were explored. The numerical results showed that the proposed analysis model was effective for calculating nonlinear behavior after cracking of curve concrete box girder bridges. There is good agreement between location and distribution of predicted crack and survey results of actual bridge. Mechanical behavior of curved box girders can be improved by taking measures such as suitably arranging bearings, reasonably setting pre-eccentricity distance of bearings, increasing reinforcement ratio.

## Introduction

Reinforced concrete(RC) box girder bridges, which have advantages of large torsional rigidity, good whole structure performance, easy construction and low cost, become a preference structural type of highway ramps and urban overpasses. Compared with straight bridges, curve bridges has curve geometric plane of girders, the supporting point of pier columns of substructure can't be located in flexural-torsional center of geometry and load of bridges.

The calculation theory of RC thin-walled curved box girders has been investigated by many scholars. More achievements have been obtained. However, the majority of them are concentrated on linear analysis of structures and simplifying the spatial problem to the simple beam calculation. It is appropriate in the condition that computer technology and analysis methods were limited ago. However, with the development of science and technology and wide application of curved box girder bridges, these design and analysis methods expose the limitation and shortage, for example, longitudinal cracking, cracking of web by principal tensile stress, local warping stress cracking, crack under anchorage or transverse crack and so on. Therefore, it is necessary that plane analysis methods are further replaced by spatial

---

<sup>1</sup>Professor, Dept. of Civil Engineering, Zhejiang University, Cyrus Tang Center for Sensor Materials and Applications, Zhejiang University, Hangzhou, 310058, China; Dept. of Civil Engineering, Zhejiang University City College, 310015, China

<sup>2</sup> Engineer, Design Institute of Highway, Zhejiang Transportation Investment Group Co., Ltd., Hangzhou, 311200, China

analysis( which may should include geometry and material nonlinearity) to analyze these cracking behavior, Concerning nonlinear analysis of RC box girder bridges, Chen & Luo (2006), based on thin-walled curved girder theory and variational principle of potential energy, deduced geometric nonlinear control differential equation. Li, etc. (2008), on the basis of Ling (1998), presented the double nonlinear coupling method to analyze nonlinear mechanical property of RC curved box girders. Yang, etc (1997) adopted stratified degradation shell elements to analyze and investigate flexural and torsional material nonlinear behavior of box girders. Duan & Zhang (2003) used finite segment method to simplify three-dimensional elastic-plastic problem into one-dimensional problem for solving it. Jan Rubeena (2010) used the commercial software to model single or multi-cell curved box girder bridges to evaluate load distribution factors. Qiao et al.(2012) deduced coupled bending torsion and shear lag of elasticity governing differential equations of curved prestressed box girder with different boundary conditions by considering prestress and initial curvature.

Above-mentioned study are focused on simplifying the structure into one-dimensional curved bar or using finite segment method, virtual layers and shell elements to simulate overall nonlinear behavior of curved box girders. The problems such as spatial nonlinear analysis theory, cracking model and parameters study of RC curved box girder bridges from elastic, cracking to failure under load have rarely been reported.

## Constitutive Model and Material Properties

### Crack Model of Concrete

Because tensile strength of concrete is low, RC structures crack at low stress level. Therefore, it generally works with cracks state under normal service load of bridges. To exactly analyze the forces of materials in reinforced RC structures of bridges, the simulation of cracks after RC structures crack is critical. At present, there are discrete crack model and smeared crack model for simulating of concrete crack. **Discrete crack model**, which uses separate elements with the cracks for boundaries, separates the surface of cracks and simulates the crack development by introducing crack interface elements and defining the relationship between the stress on the crack face and crack opening, slippage. **Smeared crack model** assumes that the concrete material after concrete cracking is still continuous and the cracks are at the state of dispersed distribution, and it simulates the crack development by using the decrease of stress and discount modulus of materials. Without updating finite element mesh dividing during the calculation and convenient analysis, the model is widely used. Smeared crack model is also adopted in the paper.

### Material Constitutive Relation

Considering the convenience of engineering application, total strain model of smeared crack models is used for concrete. Constitutive model based on total strain is obtained by expanding modified compression theory recommended by Selby and Vecchio (1993). For C50 concrete, Thorenfeldt (1987) model is adopted for compression concrete, the compressive strength is  $f_p=32.4\text{MPa}$ . Hordijk (1991) model is adopted for tensile cracks, the tensile strength is  $f_t=2.65\text{MPa}$ , fracture energy  $G_f'=0.2\text{kN/m}$ , crack width  $h=0.2\text{mm}$ , the conventional Von Mises two linear-line model is chosen for steel bars, yield strength  $f_y=335\text{MPa}$ .

## Nonlinear Analysis of Curved Box Girder Bridges

### Analysis Model

A RC curved box girder bridge is a continuous  $3 \times 20\text{m}$  highway ramp bridge. After it was open to traffic for eighteen months, many cracks occurred (Xiang, 2010, Xu, 2011). The grade of concrete is C50, HRB335 steel bar is used as main reinforcement. The distance from tensile bars centroid point to box girder top  $a_s=80.11\text{mm}$ , the area of tensile bars  $A_s=48346\text{mm}^2$ , cover thickness is 50mm, the bar rate of the whole section is 1.52%. The design load is **Super Truck- 20** and **Trailer 120** level in specification for highway bridge and culvert design in China (JTJ023-85). The curvature radius of ramp bridge  $R$  is 80m.

To analyze cracking mechanism of the RC bridge, the solid elements are used to establish 3D model of the curved box girder bridge. The bars is embedded in the model to simplify calculation model, namely, the bars are simulated by adding the stiffness of bars to parent elements. The stresses of bar are only axial, the strain  $\epsilon_{xx}$  and stress  $\sigma_{xx}$  in the integral points are calculated in tangential direction of integral points. The boundary conditions are torsional restrained in two ends and the medium piers are vertically single support on the pier columns for the bridge. There are 18480 solid elements and 27588 nodes in the model in all. In order to calculate nonlinear behaviour, here the live load of uniform lane load is exerted on the bridge. The loads are applied as equivalent nodal forces to the nodes of elements in terms of loading cases. The bending moment of mid-span in side spans is one of the most unfavorable working conditions. The lane load is eccentrically arranged.

Incremental load method is used for loading step by step and iterative computations in nonlinear analysis. The load  $P$  is step by step exerted on the bridge according to the pattern of  $P=P_d + \eta P_l$ . The load  $P_d$  is the combination of various dead actions after finished bridge, mainly including self-weight of box girder bridges and secondary dead load. The load  $P_l$  is the lane load,  $\eta$  is load factor.

For the convenience to express, the section I - I , II - II , III-III, IV-IV, V - V & VI-VI shown in Fig.1 are orderly designated in the locations of 0.5m(from bearings in side span), 9m(mid-span in side span), 15m(3/4 span in side span), 20m( middle bearings), 25m(3/4 span in central span), 30m(mid-span in central span) from left side along longitudinal direction. Besides, the points 1~11 represent the key points in the calculated section of box girder bridge, as shown in Fig. 2.

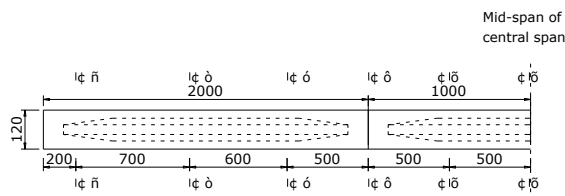


Fig. 1 Section number of bridge

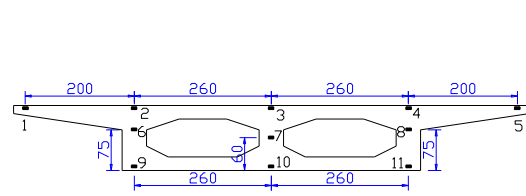


Fig. 2. Key points of the typical section  
(Dim. unit: cm)

### Load and Failure Process

According to the calculation results by the above model, Fig. 3 gives the load-deflection curves at key points in section II- II. Fig. 4 shows load-deflection distributed curve at central

point of bottom plate of box girder in the half length of whole bridge. Fig. 5 draws load-stress curves at three key points in the section II-II. Fig. 6 also shows the distribution of vertical deflection along lateral direction of bottom plate in the section II-II under different load.

The whole process of structural failure is found from Fig. 3~Fig. 6:

1) If load factor  $\eta$  ranges from 0 to 2.2, both deflection and longitudinal concrete stresses at point 1, 3, 5 in the section II-II are linearly related to exerted load, and the deflections at bottom plate of section II-II are also small. When  $\eta$  is within 1.0, the tensile stresses of concrete in the section II-II vary linearly with load increase. A few of longitudinal bending cracks appear on the bottom plate of the box girder bridge.

**Error! Reference source not found.**

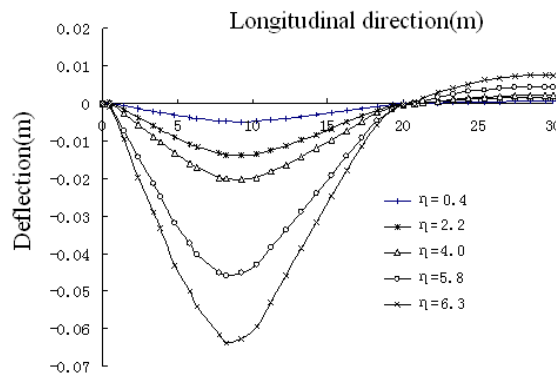


Fig. 3

Fig. 4

Fig. 3 Load-deflection curves at key points in section II-II

Fig. 4 Distribution of deflection along center line in the bottom plate of the box girder bridge under different load factors

**Error! No bookmark name given.**

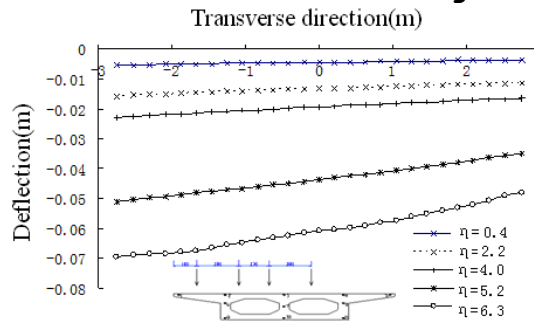


Fig. 5

Fig. 6

Fig. 5 Load-stress curves at the concrete key points in the section II-II of box girder bridge

Fig. 6 Distribution of deflection in bottom plate in the section II-II along transverse direction of box girder bridges under different load factors

2) When  $\eta > 2.2$ , there is a turnaround in the load-deflection curve, which illustrates that stiffness of concrete in the mid-span of side span significantly deteriorates. At the same time, many cracks of concrete appear on the bottom plate of box girder bridges, and concrete tensile stress doesn't increase with load any longer. Based on slight decrease of softening curve in the constitutive relation, as load increases, the bottom plate concrete of box girder bridges starts to crack. Concrete in the tensile area of the bottom plate is gradually

invalidated with the developing of crack depth. Tensile stresses of concrete near the central axis is also increasing to ultimate tensile stress until  $\eta=4.0$ . Compressive stress of concrete at point 1 of top plate located in the compressive area is generally linear changes with load in the range of  $\eta=0\sim 6$ .

3) After  $\eta>6$ , steel bar has yielded. However, there is a trend that compressive stress of concrete rapidly increases to failure. The structural stiffness sharply decreases. The deflection at point 1 in the section II-II increases suddenly. When  $\eta=6.3$ , the structure breaks to collapse. Thus, the maximum deflection in the mid-span of side span reaches 74.7mm after computation stopped.

From Fig. 6, when load factor  $\eta\leq 2.2$ , even though transverse cracks has appeared in bottom concrete of box girder, because both transverse bending stiffness and torsional stiffness of concrete are still large, the deflection of box girder along transverse direction of bottom plate is linear-uniformly distributed. When  $\eta$  is larger than or equal to 4, as longitudinal cracks of bottom plate appear in partial concrete of box girders, both transverse bending stiffness and torsional stiffness decrease, which results in significantly non-uniform distribution of deflection at the points in bottom plate along transverse direction. The vertical deflection at the side of eccentric load of curve box girder bridges is larger than that at other side. With load factor going up, the non-uniformity is more significant. This shows the influence of eccentric load and nonlinearity of concrete on the structure. At initial stage, because of low load and good integrity of the structure, the deflection is uniformly distributed. With load factor increasing, RC bridge gradually cracks and becomes nonlinear. Because of cracking of partial concrete under load, the torsional stiffness of the box girder obviously weaken and distribution of the deflection gradually trends to be non-uniform. Finally, the whole box girder bridge failures in maximum concrete stress area under eccentric load.

### Developing Process of Cracks

According to calculations under different load levels, the structure varies from elastic state to plastic state. Developing process of cracks in side span under different load levels is listed in table 1 for the bridge. As load factor increases, the side span comes into plasticity. When  $\eta$  is smaller than 0.4, positive bending moment area in the mid-span is at the elastic stage, and partial stress concentration occurs in the region nearby the side-support. When  $\eta$  is larger than or equal to 0.4, concrete in the positive bending moment area gradually varies from elasticity to plasticity. When  $\eta$  is equal to 1.0, the concrete cracks appear and gradually expand. The concrete cracks in the middle support and the positive moment area continuously expand till many cracks appear in the whole span.

Table 1 Developing process of cracks in side span of bridge under different load levels

$\eta$	Position and extent of cracking	Description of crack range(m)		
		Along the longitudinal direction*	Length	Depth
0.4	Stress concentration near side support	-	-	-
1.0	Cracks in bottom plate and web of box in the mid-span appear, crack area near side support expands, cracks near central support appear	0.25~2,7~11	1.75, 4	0.3, 0.3
2.2	Cracks in bottom plate and web of box in the mid-span are connected with those near side	0.25~13, 16.25~20	12.75, 3.75	0.6, 0.6

	support; cracks near central support expand to mid-span			
4.0	Cracks expand transversely, cracks appear in the flange in side of eccentric load; cracks at central support tend to connect with those near positive moment area	0.25~14, 16.25~20	13.75, 3.75	0.8, 0.9
6.3	Cracks expand transversely and are distributed in overall span	0.25~20	19.75	1.2

\*Note: starting from the end of girders, the range of side span in longitudinal direction is 0~20m.

In the light of the bridge field investigation results and comparison with the calculated process of crack development, it is seen that when  $\eta=1.5$ , the distribution range and average depth of the crack are relatively close to actual measured results in table 2, which illustrates that the values analyzed by the model of nonlinear prediction basically reflects actual stress state of the bridge.

Table 2 Comparison of measured values and predicted cracks distribution in side span

Bridge	Span	Average distribution range of crack in the bottom plate and web of box in side span/m			Average depth of crack in web/cm
		Inner side of box	Outboard of box	Average length	
Actual Bridge HY2	3×20m	5.0~11.0	3.8~12.6	7.4	0.51
Nonlinear calculation model		5.8~12	7.8~11.5	5.0	0.50

### Parameter Analysis of Cracking Pattern

In order to further study the influence of different parameters on cracking behavior of concrete box girder bridges, on the basis of section type and span arrangement of curved box girders studied, the parameter analysis is performed by choosing different support layouts, pre-eccentricity and reinforcement ratio etc. Element mesh dividing of analyzed model is the same with the above-mentioned one. However, analysis parameters need to be accordingly adjusted.

#### Main Reinforcement Ratio

Due to investigate the influence of main reinforcement (longitudinal reinforcement of bottom plate) ratio on the behavior of curved box girder bridges. The area of longitudinal reinforcement of bottom plate in the model with bridge radius  $R=80m$  increases or decreases 50% for parameter analysis. Table 3 lists cracking load and ultimate load with different reinforcement ratio. It is clear that the lower reinforcement ratio, the smaller cracking load and failure load.

Table 3 Comparison of cracking load and ultimate load for bridges with different reinforcement ratio

Items	Reinforcement ratio (%)		
	0.76	1.52	2.28

Cracking load in the mid-span $\eta$	0.8	1.0	1.5
Failure load $\eta$	5.4	6.3	6.9

Figure 7 shows that load-deflection curve in the section II-II with different reinforcement ratio, which illustrates that the bridge ultimate load was higher with increase of main reinforcement ratio. Clearly, the corresponding deflection under same load is smaller.

**Error! Reference source not found.**

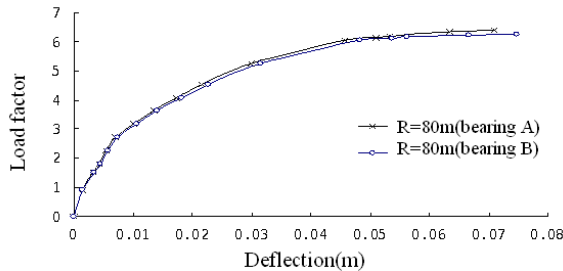


Fig. 7

Fig. 8

Fig. 7 Load-deflection curves at No.1 point

Fig. 8 Load-deflection curves with the layout pattern of different bearings

### Pattern of Support

To enhance the abilities of anti-torsion and anti-overturn, the bearings in the central pier of the curved bridge with radius  $R=80m$  are justified from type B to type A as shown in Fig. 9. The symbol “+” in the circle represents the bi-directionally movable bearing, and the symbol “-” in the circle represents the unidirectionally movable bearing. The symbol “•” in the circle represents the fixed bearing. Converged maximum load factor is up to 6.4 for type A. It is slightly bigger than type B bearing after calculations. As shown in Fig. 8, two load-deflection curves in the section II-II at the initial stage of load are approximately coincident. However, the ultimate deflection of the mid-span in the model of type A bearing in approaching to failure load is smaller than that in the model of type B bearing. Crack distribution of the side span with the layout pattern of different bearings is listed in table 4. Crack propagation of the mid-span of type A bearing lags behind that of type B bearing. In addition, distributed range and depth of cracks are slightly smaller than those in the former.

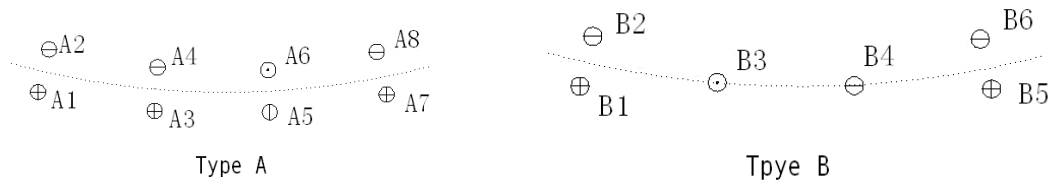


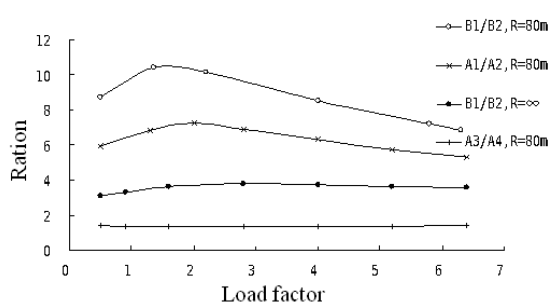
Fig. 9 Layout pattern of different bearings

Table 4 Crack distribution of the side span with the layout pattern of different bearings

Items		Crack distribution			
		Length(m)		Height(m)	
Bearing pattern		A	B	A	B
Load factor $\eta$	1.0	-,2.5	1.75,4	-,0.3	0.3,0.3
	2.2	11.0,2.5	12.75,3.75	0.6、0.4	0.6,0.6

	4.0	13.5,3.75	13.75,3.75	0.8,0.8	0.8,0.9
	6.3	19.75	19.75	1.2	1.2
Cracking load in the mid-span $\eta$		1.1	1.0		-

Fig. 10 further gives comparison of support reaction in the section IV-IV of bridges with the layout pattern of different bearings. When the quantity of bearings in second side piers changes from one bearing to two bearings, it effectively decreases the reaction of single support, enlarges the ability of anti-torsion and replaces bearings conveniently. Fig. 11 reflects that ratio of support reaction for inner side bearing and exterior bearings in straight bridges ( $B1/B2, R=\infty$ ) is significantly smaller than that in curved bridges ( $B1/B2, R=80m$ ). In other word, with the increase of radius, the inner side bearing reaction increases and the exterior bearing reaction decrease. For bearings of side piers (bearing A1, A2, B1, B2), the ratio of inner side and exterior bearings reaction in curved girder bridges ( $B1/B2, R=80m$ ) is much bigger than that in straight bridges ( $A1/A2, R=80m$ ) under equal eccentric load.



**Error! No bookmark name given.**

Fig. 10

Fig. 11

Fig. 10 Comparison of support reaction in the section IV-IV of bridges with the layout pattern of different bearings **Error! Reference source not found.**

Fig. 11 Ratio of support reaction for internal and lateral bearings in the section I - I and IV-IV of bridges with the layout pattern of different bearings

### Pre-Eccentricity Distance of Bearings on the Single Column Piers

The moment and shear forces of the curved girder bridges are close to those of the straight bridge under load except the torsion. To improve structural forces and decrease torsion, reverse moment appears by setting appropriate eccentricity to make vertical reaction of bearings on the single column pier produce eccentric moment to shear center of cross section. Because the direction of the torsion is opposite to torsion of the side span at non-eccentric state, too large torsion at the end of the girder can partially balanced.

To investigate the effect of pre-eccentric value of bearings on the single column pier on cracking pattern of box girders, the central bearing in the model is eccentric outwards, and eccentricity  $e$  is 0.0m, 0.20m, 0.40m & 0.60 m in turn. The calculated load-deflection curves are shown in Figure 12. When  $e=40cm$ , ultimate load and deflection is maximum. The condition of crack propagation in the side span with different pre-eccentricity distances is listed in Table 5. It demonstrates that cracking load and crack distribution has a certain change with the adjustment of eccentricity. At the same time, when  $e=40cm$ , the range of crack propagation under different loads is also minimum. Besides, Figure 12 and Table 5 show that adjusting eccentricity can improve the forces of the curved girder bridge. Nevertheless, too large eccentricity may result in the decrease of ultimate capacity of the

curved girder bridge. So, there is an optimal value in adjusting pre-eccentricity of the single column piers of curve box bridges.

**Error! Reference source not found.**

Fig. 12 Load-deflection curves at No.1 point in section II - II of bridges with different pre-eccentricity distance

Table 5 Crack distribution of the side span of bridges with different pre-eccentric distances

items		Crack distribution			
		Length(m)			
Pre-eccentric distance $e(m)$		0	0.2	0.4	0.6
Load factor $\eta$	1.0	1.75,4	1.25,4	1.0,4	1.5,4
	2.2	12.75,3.75	12.25,3.75	12.0,3.75	12.5,3.75
	4.0	13.75,3.75	13.0,3.75	12.75,3.75	13.5,3.75
	6.3	19.75	19.75	14.0,3.75	19.75
Cracking load in the mid-span $\eta$		1.0	1.1	1.2	1.1

### Conclusions

By the above investigations, conclusions can be drawn as follows:

Using the model that bars is embedded to the solid element of concrete, the nonlinear behavior of concrete curved box girder bridges after cracking can be calculated conveniently and effectively. The predicted crack distribution is approximately consistent with that from actual bridge investigation.

Concrete nonlinearity influences seriously deflection of box girder and distribution of support reaction of the side bearings. When external load is small, because torsional stiffness of box girders is large, transverse deflection in the girder section and support reaction for exterior bearings are approximately linearly distributed. But if load is heavy, nonlinearity of concrete box girders makes support reactions for inner side and exterior bearings tend to coincide as well.

The performance of curved box girder bridges can be enhanced by choosing the measures of appropriate bearings pattern, setting rationally pre-eccentricity of bearings on the single column pier and enhancing longitudinal reinforcement ratio of concrete etc.

For RC curved box girder bridges, especially curved girder bridge with small radius, it is suggested that designed main reinforcement ratio should be appropriately higher than that in the straight bridge and add extra torsional bars.

### Acknowledgments

This work was financially supported by Cyrus Tang Foundation and the Nation Natural Science Foundation of China (51279178).

### References

1. C. C. Guo, W. X. Wang, J.Y. Zhang etc., Optimum analysis on pre-eccentricity of single-pier point-hinged supported of curve bridges, *Urban Roads Bridges and Flood Control*, 2008(1):29-32.(in Chinese)
2. C. F. Li, W. X. Du, L. Zhou. Double nonlinear coupling analysis of reinforced concrete curve box girder, *Journal of Heilongjiang Institute of Science and Technology*, 2008, 18(5):350-354. (in Chinese)

3. D. S. Ling, J. J. Zhang, Y. Q. Xiang, et al. The method of virtual laminated element and its application in bridge engineering, *Civil Engineering Journal*, 1998 (3):22-29.(in Chinese)
4. G. H. Sun. *Calculation of curved bridge*. China Communication Press, Beijing, China,1997.
5. H. J. Duan, Q. L. Zhang. Finite segment element method for nonlinear analysis of reinforced concrete curved box girder, *Journal of Tongji University*, 2003, 31(3): 282-286. (in Chinese)
6. Hordijk, D. A. *Local approach to fatigue of concrete*. Delft, Delft University of Technology,1991
7. Jan, Rubeena, Bhat, Javed Ahmad. Evaluation of load distribution factors for curved box girder bridges, *International Journal of Earth Sciences and Engineering*, 2010,3(4):710-719.
8. J. B. Du. *Analysis of shear lag effect for continuous thin-walled curved box girder and its model experimental study*. South China University of Technology, Guangzhou, China , 2005 (in Chinese).
9. J. W. Xu. *Mechanism and control of cracking in concrete curved box girder bridges*, Zhejiang University , Hangzhou, China,2011 (in Chinese)
10. J. L. Qiao, W. L. Tian, F. Li. The analysing of coupled bending, tosion and shear-lag of curved box girder bridge considering prestress and initial curvature, *Advanced Materials Research*, 2012, Vol.446-449: 3360-3364.
11. Selby, R. G., Vecchio, F. J. *Three-dimensional constitutive relations for reinforced concrete*. Tech. Rep. 93-02, Univ. Toronto, dept. Civil Eng., Toronto, Canada, 1993
12. S. J. Zhou, Xi Zhu. Nonlinear finite element analysis and model tests of reinforced concrete box girders. *China Civil Engineering Journal*, 1996, 29(4):21-30. (in Chinese)
13. Thorenfeldt, E., Tomaszewicz, A., Jensen, J. J. Mechanical properties of high-strength concrete and applications in design, *Proceeding of Symposium on Utilization of High-Strength Concrete*, Stavanger, Norway Trondheim, 1987
14. Q. Z. Luo. Calculation of the shear lag in thin walled box girders by the finite segment method. *Journal of Hunan University*, 1991,18(2):33-38. (in Chinese)
15. Q. Y Jiang, Y. C. Ye, Z.R. Liu. Investigation on applying the smeared crack model, *China Civil Engineering Journal*, 2008, 41(2): 82-85. (in Chinese)
16. Q. Lin. *Spatial analysis of the prestressed concrete curved bridge*, Zhejiang University, Hangzhou, China (in Chinese) , 2006
17. X. Xu, D. S. Ling. Degenerated solid element series. *Journal of Solid Mechanics: Special Issue of Computational Mechanics*, 2001, (9):1-12. (in Chinese)
18. Y. P. Wu, Y. M. Lai, Y.L. Zhu, et al. Finite element method considering shear lag effect for curved box beams. *Engineering Mechanics*, 2002, 19(4): 85-59. (in Chinese)
19. Y. Q. Xiang, J.W. Xu. Crack width calculation methods of reinforced concrete bridges and application , *Proceeding of the International Symposium on Life-Cycle Performance of Bridges and Structures*, Beijing: Science Press,677-681,2010
20. Y. J. Chen, Q. Z. Luo. Nonlinear governing equation of curved box girder and its solution. *Acta Scientiarum Naturalium Universitatis Sunyatseni*, 2006, 45(5):22-25. (in Chinese)
21. Z. J. Yang, S. J. Zhou. Non-linear analysis of RC curved box girders, *China Civil Engineering Journal*, 1997, 30(3):23-39. (in Chinese)
22. *Specification for highway bridge and culvert design in China (JTJ023-85)*, China Communications Press,1986 (in Chinese)